Thin-Walled Structures 188 (2023) 110778

Contents lists available at ScienceDirect

Thin-Walled Structures

journal homepage: www.elsevier.com/locate/tws

Full length article

Thermoelastic damping in high frequency resonators using higher-order shear deformation theories

Shi-Rong Li [a,b], Feng Zhang [a], R.C. Batra [c,*]

[a] School of Civil Engineering, Nantong Institute of Technology, Nantong, Jiangsu, China
[b] School of Civil Science and Engineering, Yangzhou University, Yangzhou, Jiangsu, China
[c] Department of Biomedical Engineering and Mechanics, Virginia Polytechnic Institute and State University, Blacksburg, USA

ARTICLE INFO

Keywords:
High frequency resonators
Shear deformation beam theories
Complex frequency
Thermoelastic damping
Analytical solution

ABSTRACT

Thermoelastic damping (TED) in high frequency oscillators shifts their natural frequencies and attenuates the vibration amplitude. The amount of damping depends upon the temperature of the environment in which the device is operating. Here, we model the oscillator as a simply-supported beam of rectangular cross-section undergoing infinitesimal deformations. We consider three (the Levinson, the Timoshenko and a sinusoidal) through-the-thickness shear strain distributions, both translational and rotational inertia, and heat conduction to analytically delineate their effects on the shift in frequencies and the attenuation of their amplitudes for the lowest three vibration modes. The shear deformation distribution function multiplied by the Poisson ratio appears in the volumetric strain. The TED in the Timoshenko, the Levinson and a beam with sinusoidal variation of shear stresses is related to that in the Euler beam to recover the famous Lifshitz–Roukes formula. Various results are presented to qualitatively and quantitatively illustrate the dependence of the TED upon the lowest three frequencies and the resonator thickness. The analytical solutions presented here can be used as benchmark solutions for checking the numerical solutions.

1. Introduction

Thermoelastic damping (TED) is an inherent internal energy dissipation mechanism in resonators due to coupling between the mechanical and the thermal deformations. It originates from the irreversible flow of heat produced during cyclic deformations of resonators [1], and plays increasingly important role as the resonator dimensions are reduced. It shifts frequencies and attenuates the amplitude of vibrations from their values in homo-thermal motions. Therefore, an accurate prediction of the TED in resonators is necessary for enhancing their use as devices.

Because of the immense literature on the TED in resonators it is impossible to review all works and keep the manuscript within a reasonable length. We hope that works briefly mentioned below provide the reader a broad view of the TED in resonators.

Generally, two analytical methods have been used to evaluate the TED, namely the energy and the complex frequency method. In the energy method the inverse quality factor (Q^{-1}) is defined as the ratio of the energy dissipated in a vibration cycle to that stored in the body during its homo-thermal vibrations [2–17]. Using the energy method, Zener [2,3] established an approximate simple expression for the TED in flexural vibrations of homogeneous thin rectangular beams that was extended by Bishop and Kinra [4,5] to N-layered structures with thermally imperfect interfaces. They showed that the total internal energy loss per cycle equals the product of the total entropy produced multiplied with the equilibrium temperature. In the complex frequency method, the inverse quality factor is expressed as the ratio of the imaginary part of the complex frequency to its real part [18–51]. Lifshitz and Roukes [18] presented a closed-form solution for coupled thermomechanical vibrations of a thin beam by using the Euler–Bernoulli beam theory (EBBT) and a one-dimensional heat conduction equation.

We note that almost all structural vibration models have employed the EBBT in conjunction with either a classical [6–12,19–29,52,53] or a generalized [13–15,31–48,54] heat conduction theory. Some authors have generalized the classical EBBT to include effects of couple stresses [19,24,36,41,42,47,48,53,54] and nonlocal deformations [46–48,54].

In the framework of Fourier heat conduction theory, there have been a number of attempts to provide analytical solutions of the TED in beam resonators. Tunvir et al. [52] derived quality factors for beams of rectangular, elliptical and triangular cross-sections. Rezazadeh et al. [19] analytically analyzed plane stress/strain deformations of a beam using a modified coupled stress theory that introduces a length scale into the problem. Prabhakar and Vengallatore [6] have analyzed 2-D heat conduction in vibrating beams and expressed the

* Corresponding author.
E-mail address: rbatra@vt.edu (R.C. Batra).

https://doi.org/10.1016/j.tws.2023.110778
Received 6 March 2023; Received in revised form 9 April 2023; Accepted 11 April 2023
Available online xxxx
0263-8231/

TED as an infinite series. Zuo et al. [7] analyzed the TED in a piezoelectric beam based on the thermal energy approach. Yang and Batra [53] studied free vibrations of a linear thermo-piezo-electric body and subsequently used a perturbation method to quantify the shift in the fundamental frequency and the attenuation of its amplitude for thickness-stretch plane strain vibrations of a non-piezoelectric strip. More recently, Resmi et al. [20] have analyzed coupled thermoelastic deformations of beams by using a modified couple stress theory.

Vengllatore [8], as well as Prabhakar and Vengllatore [9] studied the TED in symmetric three-layer and asymmetric two-layer beam resonators, and numerically examined the effect of varying the volume fractions of the constituent materials. Zuo et al. [10] derived an analytical solution of the TED in an asymmetric three-layered beam. Yang et al. [11,12] investigated the TED in bilayer resonators with the top layer either fully [11] or partially [12] covered and used a 2-D heat conduction equation. Their numerical results show that peak values of the TED in the two cases occur within a range of the ratio of the thermal diffusivity of the two layers.

Khanchehgardan et al. [21] have examined effects of mass diffusion on the TED of a functionally graded material (FGM) beam resonator with the through-the-thickness variation of material properties described by a power-law function. Azizi et al. [22] investigated the TED in an FGM beam composed of silicon and a piezoelectric material and quantified effects of the volume fraction of the piezoelectric material, cross-section and ambient temperature. Zhong et al. [23] analyzed the TED in an FGM beam with material properties varying exponentially through the thickness by neglecting the stretching–bending coupling that should be considered when the material properties are asymmetric about the geometrical mid-surface. Li et al. [24] performed theoretical analyses of the TED in FGM beam resonators under different boundary conditions. For arbitrary through-the-thickness variation of the material properties, they first developed a layer-wise homogenization approach and solved the heat conduction equation with complex coefficients. Zhang and Li [25] analytically found the TED in FGM beams by considering a modified couple stress theory.

Yi and Martin [26] used the finite element method (FEM) to solve a 2-D complex eigenvalue problem derived by using a two-way coupled thermo-elasticity theory. Mendez et al. [27] have numerically investigated nonlinear thermoelastic vibrations of a cantilever beam. Utilizing an eigenvalue formulation and a customized FEM code, Guo and Yi [28] analyzed the TED in beams with square-shaped vents located along their centerlines. Guo and Yi [29] compensated for the TED in beam resonators by exploiting the piezo-resistive effect. More recently, Cheng et al. [30] numerically investigated reducing the TED in a rectangular beam by cutting slots in it of various dimensions.

In the classical heat conduction equation using Fourier's law thermal disturbances propagate at infinite speeds. Several generalized theories, e.g., the Lord–Shulman (LR), the Green–Lindsay (GL), the Green–Naghdi (GN), the dual-phase-lagging (DPL) and the three-phase lagging (TPL) theories reviewed in [31] have been proposed that provide a finite speed of propagation of thermal disturbances. Guo [32] and Guo et al. [33] derived explicit solutions of the TED in beam resonators using a single-phase lagging (SPL) and an DPL model. Abbas [34] studied the TED in a beam with the heat conduction equation having one relaxation time and fractional time derivatives. Zhou and Li [13] investigated effects of non-Fourier heat conduction on the TED in beams using the SPL model and found multiple peaks in the TED. Youssef and EI-Bary [35] employed a generalized thermo-elasticity theory with one relaxation time and two-temperature variables to deduce an explicit formula of the TED with Young's modulus varying with the reference temperature.

Vahdat et al. [36] studied the TED in a beam with piezoelectric (PZT) layers bonded on the top and the bottom surfaces by using a non-Fourier heat conduction model containing one relaxation time. They showed that imposing positive DC voltages to the PZT layers increases the critical thickness but decreases the TED while the negative DC voltage leads to the opposite trend. Bostani and Mohammdadi [37] used the energy method to obtain the analytical solution of the TED in a beam based on the LS model and a modified strain gradient elasticity theory. Utilizing the SPL heat conduction model Kumar and Mukhopadhyay derived analytical solutions of the TED in beams by applying the complex frequency method in [38] and the entropy generation approach in [14]. Kumar and Kumar investigated the TED in beam resonators by employing the TPL thermo-elasticity theory [39] and a unified formulation of the generalized coupled thermo-elasticity theories [40]. They arrived at explicit L–R formulas of the TED. Kumar et al. [41] presented the frequency shift in beams by using the TPL model for materials with memory. Borjalilou et al. [42] derived the Q^{-1} based on the modified couple stress and the DPL heat conduction equation by the complex frequency approach. Borjalilou and Asghari [43] extended the work reported in [42] by including effects of electrical actuation. Guha and Singh [44] studied beams containing sandiness and voids based on both the LS and GL generalized heat conduction theories, and Kaur et al. [45] considered transversely isotropic beams and used the GN III theory. Shi et al. [15] have presented a closed-form expression for the TED in transversely isotropic material beams by considering the size-dependent and the surface effects in the DPL theory.

The TED considering nonlocal effects based on Eringen's theory [54] have been investigated in [46–49]. Kumar and Mukhopadhyay [46] considered both the size-dependence and the nonlocal effects in the SPL model with the modified couple stress theory. Using the DPL heat conduction equation, Borjalilou et al. [47] examined the TED by considering nonlocal effects. Kaur et al. [48] employed a generalized piezo-thermo-elasticity theory with two temperatures and nonlocal Eringen's constitutive relations to analyze the TED. Gu et al. [49] used the DPL generalized thermo-elasticity theory to investigate the nonlocal, the surface and the thermal relaxation effects on the TED.

Like higher-order strain gradients in the mechanical problem Batra [55] considered 2nd order spatial and spatial time derivatives in the internal energy equation for a rigid heat conductor. He showed that thermal waves propagate at a finite speed. The linearized heat equation has four relaxation times and two thermal conductivities one of which depends upon a length parameter. Cattaneo [56] and Chester [57] have proposed heat equations that permit finite speeds of thermal waves.

Nearly all works cited above are based on the EBBT. However, a few authors have analyzed the TED in either thick or short beams with either the Timoshenko (TBT) or the first-order shear deformation theory (FSDT) [16,17,50,51]. Parayil et al. [16] used the FSDT to find an approximate solution of 2-dimensional thermo-mechanical deformations of a beam and considered in [17] geometrical nonlinearities due to bending-stretching deformations of the mid-plane and the actuating electrostatic force. Rezazadeh et al. [50] studied the TED in electrostatically deflected short beams based on Eringen's nonlocal elasticity theory and the DPL heat conduction model. Emami and Alibeigloo [51] analyzed the TED in an FGM Timoshenko beam with the through-the-thickness variation of material properties described by a power law function. The eigenvalue problem with complex frequencies was solved by using Navier's method and the $Q^{-1}$was extracted.

In the EBBT effects of transverse shear deformations and rotational inertia on the transient response are neglected, and the TBT gives a uniform through-the-thickness distribution of the transverse shear stress that violates vanishing of tangential tractions on the top and the bottom surfaces of a beam either loaded by only normal or null tractions on these surfaces. This has been corrected to a large extent in higher-order shear deformation theories (HSDTs) [58–61] that provide null tangential tractions on major surfaces of a beam, and need modifications to satisfy non-zero tangential tractions applied on these surfaces. The modifications have been made in plate/beam theories proposed in [62–65] and in other papers not cited here. The Carrera Unified Formulation (CUF) for micropolar plates is described in [64] and for the analysis of thermoelastic deformations of beam-type structures in [65]. The Carrera plate/shell/beam theories, Batra and Vidoli's plate theories [66] and various other higher-order shear deformation

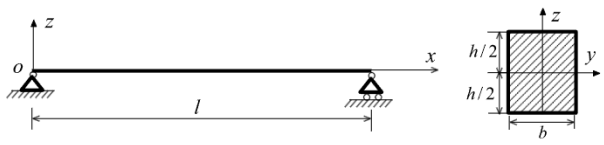

Fig. 1a. Geometry and supports of a rectangular cross-section beam and the Cartesian coordinate axes.

theories (HSDTs) [58–60] can be deduced from Mindlin's theories [67]. Batra and Vidoli [63] have studied deformations of a cantilever beam with tangential tractions applied on its top and bottom surfaces. Qian and Batra [68] have analyzed transient thermoelastic deformations of a thick plate. However, they did not consider the TED. Plate theories using classical linear elasticity concepts have been extended to those using strain gradients as kinematic variables and the associated couple stresses as kinetic variables; e.g., see [67]. Like micropolar theories these involve a length scale that helps mitigate effects of the finite element mesh while numerically solving the governing equations. A length scale also appears in Eringen's non-local theory [46–49,54] that expresses stresses at a point in terms of strains averaged over a domain centered at the point of interest. Higher-gradient and micro-inertia effects have been considered in analyzing composite beam structures by Ayad et al. [69] who found values of material characteristics length using a homogenization theory for a beam made of alternate thin blocks of two materials. They found that the vibration frequency depends upon the wave number.

As far as we can ascertain the TED has not been analyzed using the Levinson and a sinusoidal through-the-thickness shear stress distribution. It could certainly be numerically studied but that will not provide closed-form expressions for the frequency shift and the amplitude attenuation.

The novelty of the work is to provide closed-form expressions for the TED-induced change in the frequencies and amplitudes of vibration of a simply-supported beam of rectangular cross-section. This will be useful to resonator designers at least in arriving at preliminary designs that could be improved upon by numerically analyzing either their 3-dimensional thermo-mechanical deformations or employing CUF-based analysis with higher-order beam/plate theories. The closed-form expression given here for the inverse quality factor Q^{-1} will serve as a benchmark against which numerical solutions could be compared. Numerical solutions could consider dependence of material properties upon the temperature and the geometric/material nonlinearities.

Here, we consider three through-the-thickness distributions of the shear stress to delineate the TED in beams of various length/thickness (or aspect) ratios. Assuming that the heat conduction effects are dominant in the beam thickness direction, we analytically find an expression for the through-the-thickness variation of the temperature. The main results of the paper are (i) providing an expression for the complex frequency of free vibration of a shear deformable beam in terms of that of the EB beam, and (ii) quantifying the TED in shear deformable beams. Numerical results listed and plotted in the paper compare the TED values for three different shear stress shape functions with that for the EBBT for different values of the aspect ratio.

2. Equations of motion

Consider a simply supported beam resonator of rectangular cross-section having length l, height h and width b schematically shown in Fig. 1 where the rectangular Cartesian coordinate axes employed to study its infinitesimal thermo-mechanical deformations are also exhibited. Thus, the beam's neutral surface is the x-y plane and the positive z-axis points upwards along the thickness direction. The beam material is assumed to be isotropic, homogeneous and linearly elastic, and the displacement field used for a higher-order shear deformation beam theory (HSDT) is given by [59,61]

$$u(x,z,t) = -z\frac{\partial w_0}{\partial x} + f(z)\varphi(x,t) \tag{1a}$$

Table 1
Four stress shape functions, $f(z)$. and the corresponding stress functions $g(z)$.

Function type	$f(z)$	$g(z)$
Polynomial	$z - \frac{4z^3}{3h^2}$	$1 - \frac{4z^2}{h^2}$
Trigonometric	$\frac{h}{\pi}\sin\left(\frac{\pi z}{h}\right)$	$\cos\left(\frac{\pi z}{h}\right)$
Hyperbolic	$\frac{\pi z - h\sinh(\pi z/h)}{\pi[\cosh(\pi/2) - 1]} + z$	$\frac{1-\cosh(\pi z/h)}{\cosh(\pi/2)-1} + 1$
Exponential	$ze^{-2(z/h)^2}$	$e^{-2(z/h)^2}\left(1 - 4\frac{z^2}{h^2}\right)$

$$w(x,z,t) = w_0(x,t) \tag{1b}$$

where w_0 is the beam deflection, φ a rotation about the y-axis of the transverse normal, and $f(z)$ a shape function defining through-the-thickness variation of the transverse shear strains and stresses satisfying zero tangential tractions on the top and the bottom surfaces except for the TBT for which $f(z) = z$. The function $f(z)$ need not be a polynomial function of z. For example, it may be a trigonometric, a hyperbolic, an exponential or a logarithmic function. Four choices of $f(z)$ and their corresponding shear stress functions $g(z) = \mathrm{d}f/\mathrm{d}z$ are listed in Table 1 and plotted in Fig. 1b.

The non-zero axial strain ε_x and the transverse shear strain γ_{xz} found from Eq. (1a,b) are

$$\varepsilon_x = -z\frac{\partial^2 w_0}{\partial x^2} + f(z)\frac{\partial \varphi}{\partial x} \tag{2a}$$

$$\gamma_{xz} = g(z)\varphi \quad \text{with} \quad g(z) = \frac{\mathrm{d}f}{\mathrm{d}z} \tag{2b}$$

The axial stress σ_x and the transverse shear stress τ_{xz}, found using Hooke's law, are

$$\sigma_x = E\left[-z\frac{\partial^2 w_0}{\partial x^2} + f(z)\frac{\partial \varphi}{\partial x}\right] - E\alpha\theta \tag{3}$$

$$\tau_{xz} = \frac{Eg(z)}{2(1+\nu)}\varphi \tag{4}$$

where $\theta(x,y,z,t) = T(x,y,z,t) - T_0$ is the temperature change, and T_0 is the reference temperature. Moreover, E, ν and α, respectively, are Young's modulus, Poisson's ratio and the coefficient of thermal expansion. The axial thermal strain equals $\alpha\theta$.

Assuming that the top and the bottom surfaces of the beam are traction free and thermally insulated, we write equations of motion (5)–(7) in terms of the resultant shear force F_S, and the moment M about the y-axis.

$$\frac{\partial M}{\partial x} - F_s = \frac{\partial^2}{\partial t^2}\left(-I_2\frac{\partial w_0}{\partial x} + I_{f1}\varphi\right) \tag{5}$$

$$\frac{\partial F_s}{\partial x} = I_0\frac{\partial^2 w_0}{\partial t^2} \tag{6}$$

$$(F_S, M) = b\int_{-h/2}^{h/2}(\tau_{xz}, \sigma_x z)\mathrm{d}z \tag{7}$$

The inertial parameters I_0, I_2 and I_{f1} in Eqs. (5) and (6) are defined as

$$I_0 = \rho bh,\quad I_2 = \rho bh^3/12,\quad I_{f1} = b\rho\int_{-h/2}^{h/2} f(z)z\mathrm{d}z \tag{8}$$

where ρ is the mass density (kg/m^3). Substitution of Eqs. (3) and (4) into Eq. (7) yields

$$M = -S_2\frac{\partial^2 w_0}{\partial x^2} + S_{f1}\frac{\partial \varphi}{\partial x} - M_T,\quad F_s = S_g\varphi \tag{9a,b}$$

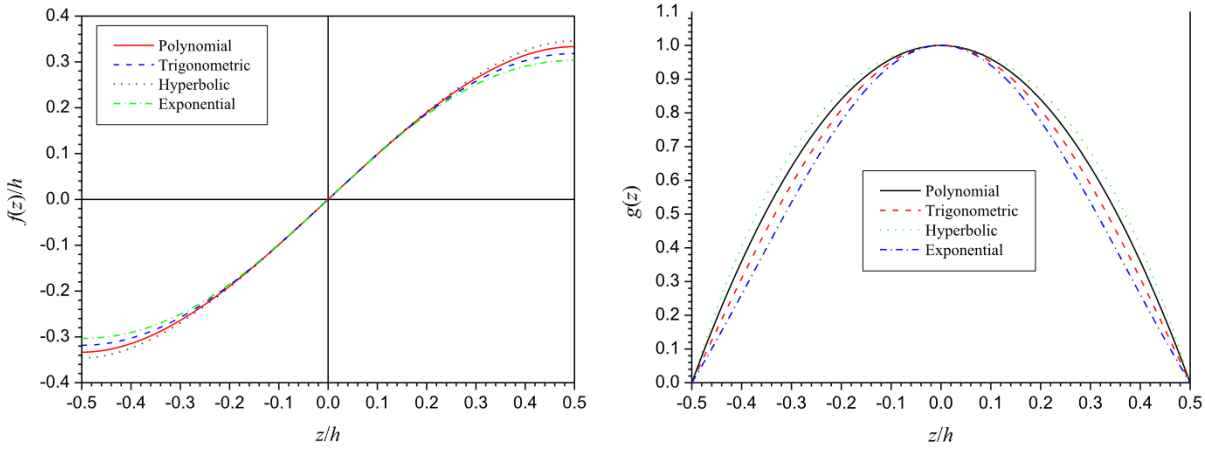

Fig. 1b. Through-the-thickness variations of four choices of function $f(z)$ and $g(z) = \mathrm{d}f/\mathrm{d}z$.

where

$$S_2 = \frac{Ebh^3}{12}, S_{f1} = bE\int_{-h/2}^{h/2} f(z)z\mathrm{d}z, S_g = \frac{Eb}{2(1+\nu)}\int_{-h/2}^{h/2} g(z)\mathrm{d}z,$$

$$M_T = \alpha bE\int_{-h/2}^{h/2} \theta z\mathrm{d}z \tag{10a,b,c,d}$$

The thermal bending moment M_T produced by the temperature change is calculated from the thermal stress $\alpha E\theta$.

Substitution for M and F_S from Eq. (9) into Eqs. (5) and (6) gives differential equations (11) and (12) governing free vibrations of the beam in terms of the functions w_0 and φ.

$$-S_2\frac{\partial^3 w_0}{\partial x^3} + S_{f1}\frac{\partial^2\varphi}{\partial x^2} - \frac{\partial M_T}{\partial x} - S_g\varphi = \frac{\partial^2}{\partial t^2}\left[-I_2\frac{\partial w_0}{\partial x} + I_{f1}\varphi\right] \tag{11}$$

$$\frac{\partial\varphi}{\partial x} = \frac{I_0}{S_g}\frac{\partial^2 w_0}{\partial t^2} \tag{12}$$

We now substitute for φ from Eq. (12) into Eq. (11) to obtain the differential equation for the deflection w_0.

$$S_2\frac{\partial^4 w_0}{\partial x^4} + \frac{\partial^2 M_T}{\partial x^2} = -\frac{\partial^2}{\partial t^2}\left[I_0 w_0 - \left(I_2 + \frac{I_0 S_{f1}}{S_g}\right)\frac{\partial^2 w_0}{\partial x^2} + \frac{I_0 I_{f1}}{S_g}\frac{\partial^2 w_0}{\partial t^2}\right] \tag{13}$$

The temperature change, θ, appearing in Eq. (10d) is found by solving the heat conduction equation as discussed below.

3. Heat conduction equation

The evolution of temperature, θ, in an isotropic and homogeneous beam is governed by Eq. (14); e.g., see [1].

$$\kappa\left(\frac{\partial^2\theta}{\partial x^2} + \frac{\partial^2\theta}{\partial z^2}\right) = \rho C\frac{\partial\theta}{\partial t} + \frac{\alpha E T_0}{1-2\nu}\frac{\partial\varepsilon_{ii}}{\partial t} \tag{14}$$

In Eq. (14) κ is the thermal conductivity, C the specific heat, and the dilatation ε_{ii} given by [Eqs. 9 and 10 of Ref. [18]] is

$$\varepsilon_{ii} = \varepsilon_{xx} + \varepsilon_{yy} + \varepsilon_{zz} = (1-2\nu)\left[-z\frac{\partial^2 w_0}{\partial x^2} + f(z)\frac{\partial\varphi}{\partial x}\right] + 2(1+\nu)\alpha\theta \tag{15}$$

For small amplitude transverse vibrations of the beam we assume that heat conduction effects are dominant in the beam thickness direction, or $\left|\frac{\partial^2\theta}{\partial x^2}\right| << \left|\frac{\partial^2\theta}{\partial z^2}\right|$. We substitute from Eq. (15) into Eq. (14), neglect the term $\frac{\partial^2\theta}{\partial x^2}$ on the left-hand side of Eq. (14), and get

$$\kappa\frac{\partial^2\theta}{\partial x^2} = \rho C\left(1 + \frac{2(1+\nu)\alpha^2 E T_0}{(1-2\nu)\rho C}\right)\frac{\partial\theta}{\partial t} + \alpha E T_0\frac{\partial}{\partial t}\left[-z\frac{\partial^2 w_0}{\partial x^2} + f(z)\frac{\partial\varphi}{\partial x}\right] \tag{16}$$

Boundary conditions for a simply-supported (S-S) beam with the top and the bottom surfaces thermally insulated are

$$w_0 = 0, M = 0 \quad \text{on} \quad x = 0, l \tag{17a}$$

$$\frac{\partial\theta}{\partial z} = 0 \quad \text{on} \quad z = \pm h/2 \tag{17b}$$

No boundary conditions for the temperature are needed at $x = 0, l$, and no initial conditions are needed to study free vibrations of the beam.

4. Harmonic response of the system

Assuming that free vibrations of the beam are harmonic and the kinematic parameters together with the temperature change have the same complex-valued frequency ω, we write

$$(w_0, \theta) = \left(\overline{w}, \overline{\theta}\right)\mathrm{e}^{\mathrm{i}\omega t} \tag{18}$$

where $i = \sqrt{-1}$; $\overline{w}$ and $\overline{\theta}$ are, respectively, amplitudes of vibrations of w_0 and θ. The real part of ω determines the oscillatory motion and the imaginary part the attenuation of the amplitude of vibration. Substitution from Eq. (18) into Eqs. (13) and (16) yields the following eigenvalue problem:

$$S_2\frac{\mathrm{d}^4\overline{w}}{\mathrm{d}x^4} + \overline{\phi}_2\frac{\mathrm{d}^2\overline{w}}{\mathrm{d}x^2} + \overline{\phi}_0\overline{w} + \frac{\mathrm{d}^2\overline{M}_T}{\mathrm{d}x^2} = 0 \tag{19}$$

$$\frac{\partial^2\overline{\theta}}{\partial z^2} = \frac{\mathrm{i}\omega}{\chi}\left\{\overline{\theta} + \frac{\Delta_E}{\alpha}\left[-z\frac{\mathrm{d}^2\overline{w}}{\mathrm{d}x^2} + f(z)\frac{\mathrm{d}\overline{\phi}}{\mathrm{d}x}\right]\right\} \tag{20}$$

in which

$$\overline{\phi}_0 = \omega^2 I_0\left(\omega^2\frac{I_{f1}}{S_g} - 1\right), \ \overline{\phi}_2 = \omega^2 I_0\left[\frac{I_2}{I_0} + \frac{S_{f1}}{S_g}\right], \ \overline{M}_T = \alpha bE\int_{-h/2}^{h/2}\overline{\theta}z\mathrm{d}z \tag{21a,b,c}$$

$$\Delta_E = E\alpha^2 T_0/(\rho C), \chi = \kappa/(\rho C) \tag{21d,e}$$

Henceforth, we use the following non-dimensional variables related to their dimensional counterparts by Eq. (22).

$$(X, W) = (x, \overline{w})/l, \quad (\zeta, \lambda) = (z, l)/h \tag{22a}$$

$$\Theta = \alpha\overline{\theta}, \quad m_T = l\overline{M}_T/S_2, \quad F(\zeta) = f(z)/h, \quad \Omega = l^2\omega\sqrt{I_0/S_2} \tag{22b}$$

Substituting from Eq. (22) into Eqs. (19) and (20), we get governing equations (23) and (24) in terms of non-dimensional variables.

$$\frac{\mathrm{d}^4 W}{\mathrm{d}X^4} + \phi_2\Omega^2\frac{\mathrm{d}^2 W}{\mathrm{d}X^2} + (\phi_{02}\Omega^2 - 1)\Omega^2 W + \frac{\mathrm{d}^2 m_T}{\mathrm{d}X^2} = 0 \tag{23}$$

Table 2
Normalized values of c_s and c_f for the three shape functions $f(z)$.

$f(z)$	$F(\zeta)$	$g(z)$	$\frac{\lambda^2}{1+\nu}c_s$	c_f
$f_1 = z$	$F_1 = \zeta$	1	1/5	1
$f_2 = z - \frac{4z^3}{3h^2}$	$F_2 = \zeta - \frac{4\zeta^3}{3}$	$1 - \frac{4z^2}{h^2}$	$\frac{1}{4}$	$\frac{4}{5}$
$f_3 = \frac{h}{\pi}\sin\left(\frac{\pi z}{h}\right)$	$F_3 = \frac{1}{\pi}\sin(\pi\zeta)$	$\cos\left(\frac{\pi z}{h}\right)$	$\frac{\pi}{12}$	$\frac{24}{\pi^3}$

$$\frac{\partial^2\Theta}{\partial\zeta^2} + p^2\overline{\Theta} = p^2 q\left(\zeta\frac{\mathrm{d}^2W}{\mathrm{d}\xi^2} + c_s\Omega^2 F(\zeta)W\right) \tag{24}$$

where

$$\phi_{02} = \frac{c_s c_f}{12\lambda^2},\quad \phi_2 = \frac{1}{12\lambda^2} + c_s c_f,\quad c_s = \frac{S_2}{l^2 S_g}, c_f = \frac{S_{f1}}{S_2} \tag{25a}$$

$$g = \lambda^2\chi\sqrt{\frac{I_0}{S_2}},\quad q = \frac{\Delta_E}{\lambda\alpha},\quad p = \sqrt{-\mathrm{i}\frac{\Omega}{g}} \tag{25b}$$

Dimensionless parameters c_s and c_f are related to the shear deformation shape function $f(z)$ and the aspect ratio, $\lambda = l/h$, of the beam.

Herein, we study the problem for three choices, namely linear, cubic polynomial and sinusoidal, of function $f(z)$ listed in Table 1. The corresponding function $g(z)$ and the two parameters, c_s and c_f defined in Eq. (25a), are also listed in Table 2. The choice $f(z) = z$ reduces the beam theory to Timoshenko's or the FSDT that does not satisfy the vanishing of the shear tractions on beam's top and bottom surfaces. Thus, we employ the shear stiffness coefficient $F_S = k_s\int_{-h/2}^{h/2}\tau_{xz}\mathrm{d}z$, where $k_s = 5/6$ is the shear correction factor for a rectangular cross section. The other two choices for $f(z)$ are for HSDTs and satisfy $\tau_{xz}|_{z=\pm h/2} = 0$. The choice of a cubic polynomial for $f(z)$ results in through-the-thickness parabolic distribution of the transverse shear stress and has been widely used in studying static and dynamic deformations of beams; e.g., see [51,58–61]. The governing equations for $f(z) = 0$ reduce to those for the EBBT.

5. Complex frequency and TED

Corresponding to the above three choices for $f(z)$ the general solutions of the heat conduction Eq. (24) are listed below as Eqs. (26), (27) and (28).

$$\Theta_1 = A_1\sin(p\zeta) + B_1\cos(p\zeta) + q\left(\zeta\frac{\mathrm{d}^2W}{\mathrm{d}X^2} + c_s\Omega^2 F_1(\zeta)W\right) \tag{26}$$

$$\Theta_2 = A_2\sin(p\zeta) + B_2\cos(p\zeta) + q\left[\zeta\frac{\mathrm{d}^2W}{\mathrm{d}X^2} + c_s\Omega^2\left(\frac{8\zeta}{p^2} + F_2(\zeta)\right)W\right] \tag{27}$$

$$\Theta_3 = A_3\sin(p\zeta) + B_3\cos(p\zeta) + q\left(\zeta\frac{\mathrm{d}^2W}{\mathrm{d}X^2} + \frac{c_s p^2\Omega^2}{p^2-\pi^2}F_3(\zeta)W\right) \tag{28}$$

Here $F_i(\zeta)$ for $i = 1,2,3$ are non-dimensional forms of $f_i(z)$ listed in Table 1. Constants A_i and B_i $(i = 1,2,3)$ are found from

$$\left.\frac{\partial\Theta}{\partial\zeta}\right|_{\zeta=\pm1/2} = 0 \tag{29}$$

that is Eq. (17b) written in non-dimensional variables. We thus get

$$\Theta_1 = q\left(\zeta - \frac{\sin(p\zeta)}{p\cos(p/2)}\right)\left(\frac{\mathrm{d}^2W}{\mathrm{d}X^2} + c_s\Omega^2 W\right) \tag{30}$$

$$\Theta_2 = q\left(\zeta - \frac{\sin(p\zeta)}{p\cos(p/2)}\right)\left(\frac{\mathrm{d}^2W}{\mathrm{d}X^2} + \frac{8c_s}{p^2}\Omega^2 W\right) + qc_s\Omega^2 F_2(\zeta)W \tag{31}$$

$$\Theta_3 = q\left(\zeta - \frac{\sin(p\zeta)}{p\cos(p/2)}\right)\frac{\mathrm{d}^2W}{\mathrm{d}X^2} + \frac{qp^2c_s\Omega^2}{p^2-\pi^2}F_3(\zeta)W \tag{32}$$

Substitution from Eqs. (30)–(32) in the dimensionless form of Eq. (10d) gives

$$m_T = \mu_1\frac{\mathrm{d}^2W}{\mathrm{d}\xi^2} + \mu_2 c_s\Omega^2 W \tag{33}$$

where

$$\mu_1 = \lambda q\psi,\quad \psi = 1 + \frac{24}{p^3}\left(\frac{p}{2} - \tan\frac{p}{2}\right) \tag{34}$$

$$\mu_2 = \begin{cases}\lambda q\psi & \text{for } F_1\\ \lambda q\left(\frac{4}{5} + \frac{8}{p^2}\psi(\Omega)\right) & \text{for } F_2\\ \frac{24\lambda q p^2}{\pi^3(p^2-\pi^2)} & \text{for } F_3\end{cases} \tag{35}$$

Furthermore, substitution of Eq. (33) into Eq. (23) gives

$$(1+\mu_1)\frac{\mathrm{d}^4W}{\mathrm{d}X^4} + (\phi_2 + c_s\mu_2)\Omega^2\frac{\mathrm{d}^2W}{\mathrm{d}X^2} + (\phi_{02}\Omega^2 - 1)\Omega^2 W = 0 \tag{36}$$

for W. By using Eqs. (9), (22) and (34) the dimensionless bending moment can be written as

$$m = \frac{Ml}{S_2} = -(1+\mu_1)\frac{\mathrm{d}^2W}{\mathrm{d}X^2} - (c_f + \mu_2)c_s\Omega^2 W \tag{37}$$

To solve differential Eq. (36), we use boundary conditions (17a) that in terms of non-dimensional variables are

$$W(0) = W(1) = 0,\quad m(0) = m(1) = 0 \tag{38}$$

The function $W = A_n\sin(n\pi X)$ $(n = 1,2,\ldots)$ satisfies Eqs. (36) and (38) provided that

$$\phi_{02}\Omega^4 - [1 + (\phi_2 + c_s\mu_2)\Omega_{\mathrm{E}0}]\Omega^2 + (1+\mu_1){\Omega_{\mathrm{E}0}}^2 = 0 \tag{39}$$

Here Ω is the dimensionless complex natural frequency of the simply-supported beam and $\Omega_{\mathrm{E}0} = n^2\pi^2$ is the natural frequency of the Euler–Bernoulli (E–B) beam for a mechanical problem.

From Eqs. (25), (34) and (35) it can be seen that Eq. (39) is a nonlinear transcendental equation for Ω because $\mu_1(\Omega)$ and $\mu_2(\Omega)$ are transcendental functions of Ω. To simplify the calculation, as it has been done in the literature, these functions are evaluated at $\Omega = \Omega_0$ where Ω_0 is the natural frequency of the beam under isothermal conditions. With this approximation, an analytical solution of Eq. (39) is

$$\Omega = \left(\frac{1 + (\phi_2 + c_s\mu_2)\Omega_{\mathrm{E}0} \pm \sqrt{[1 + (\phi_2 + c_s\mu_2)\Omega_{\mathrm{E}0}]^2 - 4\phi_{02}(1+\mu_1){\Omega_{\mathrm{E}0}}^2}}{2\phi_{02}}\right)^{1/2} \tag{40}$$

The isothermal frequency Ω_0 is first found by setting $\mu_1 = \mu_2 = 0$ in Eq. (40), then the energy dissipation parameters μ_1 and μ_2 are calculated by using Eqs. (34) and (35), and the complex frequency Ω is found from Eq. (40). The inverse quality factor [18] of the S-S beam is determined from

$$Q^{-1} = 2\left|\frac{\mathrm{Im}(\Omega)}{\mathrm{Re}(\Omega)}\right| \tag{41}$$

in which $\mathrm{Re}(\Omega)$ and $\mathrm{Im}(\Omega)$ are the real and the imaginary parts of Ω.

By setting $f(z) = 0$ in Eq. (1), or equivalently $\phi_{02} = \phi_2 = c_s = 0$ in Eq. (39), we get the complex frequency Ω_{E} of the E–B beam as

$$\Omega_{\mathrm{E}} = \Omega_{\mathrm{E}0}\sqrt{1 + \mu_1(\Omega_{\mathrm{E}0})} \approx \Omega_{\mathrm{E}0}[1 + \mu_1(\Omega_{\mathrm{E}0})/2] \tag{42}$$

From Eq. (42) we can derive the well-known Lifshitz–Roukes (L–R) [18] expression for the E–B beam

$$Q_{\mathrm{E}}^{-1} = \frac{6\Delta_E}{\xi^2}\left(1 - \frac{1}{\xi}\frac{\sinh\xi + \sin\xi}{\cosh\xi + \cos\xi}\right) \tag{43}$$

where $\xi = h\sqrt{\omega_{\mathrm{E}0}/(2\chi)}$, $\omega_{\mathrm{E}0} = \Omega_{\mathrm{E}0}\sqrt{S_2/I_0}/l^2$ is the homo-thermal frequency of the E–B beam, and Δ_E is given by Eq. (21d).

Table 3
Material properties at $T_0 = 300$ K.

Materials	E (GPa)	ρ (kg/m^3)	κ (W/m/K)	C (J/kg/K)	α (10^{-6}/K)	ν
SiC	427	3100	65	670	4.3	0.17
Ni	210	8900	92	438.2	13.0	0.3

Table 4
First two non-dimensional frequencies (Ω_0) for isothermal deformations of E - B and shear-deformable beams (Poisson's ratio, $\nu = 0.3$).

n	$F(\zeta)$	λ							
		50	30	10	9	8	7	6	5
1	0	9.8696	9.8696	9.8696	9.8696	9.8696	9.8696	9.8696	9.8696
	F_1	9.8629	9.8511	9.7075	9.6709	9.6205	9.5488	9.4420	9.2740
	F_2	9.8629	9.8511	9.7075	9.6709	9.6205	9.5488	9.4419	9.2740
	F_3	9.8629	9.8509	9.7059	9.6689	9.6181	9.5457	9.4380	9.2686
2	0	39.478	39.478	39.478	39.478	39.478	39.478	39.478	39.478
	F_1	39.372	39.185	37.096	36.609	35.965	35.094	33.886	32.167
	F_2	39.372	39.185	37.096	36.609	35.965	35.094	33.886	32.167
	F_3	39.371	39.182	37.075	36.583	35.934	35.057	33.842	32.113

6. Through-the-thickness temperature variation

Bu substituting $W = A_1 \sin(\pi X)$ into Eqs. (30)–(32) we get the following expression for the non-dimensional temperature change

$$\Theta_i = H_i(\zeta) W_n(X), \quad (i = 1, 2, 3) \tag{44}$$

where function $H_i(\zeta)$ represents the variation of $\Theta_i(\zeta)$ across the beam thickness. Corresponding to the three shear functions listed in Table 1, functions $H_i(\zeta)$ are

$$H_1(\zeta) = H_E(\zeta) + c_s q \Omega^2 \left(\zeta - \frac{\sin(p\zeta)}{p\cos(p/2)} \right), \quad c_s = \frac{1+\nu}{5\lambda^2} \tag{45}$$

$$H_2(\zeta) = H_E(\zeta) + c_s q \Omega^2 \left[\frac{8}{p^2} \left(\zeta - \frac{\sin(p\zeta)}{p\cos(p/2)} \right) + F_2(\zeta) \right], \quad c_s = \frac{1+\nu}{4\lambda^2} \tag{46}$$

$$H_3(\zeta) = H_E(\zeta) + \frac{c_s q p^2 \Omega^2}{p^2 - \pi^2} F_3(\zeta), \quad c_s = \frac{(1+\nu)\pi}{12\lambda^2} \tag{47}$$

where

$$H_E(\zeta) = -(n\pi)^2 q \left(\zeta - \frac{\sin(p\zeta)}{p\cos(p/2)} \right) \tag{48}$$

is for the EBBT. For $c_s = 0$, shearing deformations vanish and Eqs. (45)–(47) reduce to Eq. (48).

7. Numerical results and discussions

In this section, we investigate the effect of shear deformations on the TED for silicon carbide (SiC) and nickel (Ni) beams; values of the material parameters are listed in Table 3.

By setting $\mu_1 = \mu_2 = 0$ in Eq. (40) we obtain expressions for the non-dimensional frequency, Ω_0, of an S-S shear deformable beam without considering the TED. Two lowest frequencies for various values of the aspect (length/height = λ) ratio are provided in Table 4. A comparison of frequencies for different values of the function $F(\zeta)(F = 0$ for the E–B beam) reveals that for a fixed λ the consideration of shear deformations decreases the frequency from that of the E–B beam. For each value of λ the first two frequencies do not depend upon the through-the-thickness shear distribution because parameters ϕ_{02} and ϕ_2 in Eq. (23) are the same for $m_T = 0$. Furthermore, the effect of shear deformation diminishes with an increase in λ and becomes negligible for $\lambda = 50$, and equals ~2% for $\lambda = 10$.

We could not find in the open literature the inverse quality factors of beams based on the HSDTs used here. We list in Table 4 for some values of λ the first two frequencies for the EBBT ($F = 0$) and the FSDT ($F = F_1$). The values of inverse quality factor corresponding to the first two vibration modes for the E–B beam are calculated using the L–R solution [18], Eq. (43). From the results listed in Table 5 it is evident that values of Q^{-1} estimated by the FSDT and the HSDT are less than those given by the EBBT and the relative error between them increases with a decrease in λ. Moreover, the effect of shear deformation on the TED related to the second mode is more than that related to the first mode.

Table 5
Inverse quality factor ($Q^{-1} \times 10^4$) of the two beams using different shear deformable functions in beam theories ($h = 1$ μm).

(a) SiC beam									
n	$F(\zeta)$	λ							
		50	30	10	9	8	7	6	5
1	0	0.4865	1.3346	5.6174	5.4103	4.9480	4.2540	3.4077	2.5204
	F_1	0.4857	1.3289	5.4967	5.2880	4.8306	4.1466	3.3121	2.4351
	F_2	0.4857	1.3289	5.4953	5.2865	4.8291	4.1454	3.3116	2.4364
	F_3	0.4857	1.3288	5.4936	5.2847	4.8273	4.1436	3.3100	2.4351
2	0	1.8928	4.3984	2.5204	2.0953	1.6966	1.3310	1.0024	0.7135
	F_1	1.8814	4.3348	2.4351	2.0142	1.6193	1.2578	0.9346	0.6531
	F_2	1.8813	4.3343	2.4364	2.0169	1.6241	1.2652	0.9452	0.6671
	F_3	1.8928	4.3334	2.4351	2.01587	1.6233	1.2649	0.9453	0.6677
Ni beam									
1	0	0.6403	1.7719	11.841	12.862	13.452	13.252	11.984	9.7017
	F_1	0.6392	1.7635	11.488	12.383	12.899	12.663	11.414	9.1997
	F_2	0.6392	1.7635	11.445	12.380	12.894	12.656	11.407	9.1944
	F_3	0.6392	1.7634	11.440	12.373	12.887	12.648	11.399	9.1864
2	0	2.5397	6.6546	9.7017	8.3164	6.8773	5.4670	4.1534	2.9809
	F_1	2.5226	6.5364	9.1998	7.8560	6.4575	5.0843	3.8048	2.6690
	F_2	2.5224	6.5355	9.1944	7.8530	6.4585	5.0918	3.8224	2.7009
	F_3	2.5222	6.5340	9.1865	7.8457	6.4521	5.0866	3.8190	2.6998

Values of the inverse quality factor, Q^{-1}, listed in Table 5 reveal that the shear deformations affect the TED for all values of λ considered. For example, for $\lambda = 5$ and the shear deformations described by functions F_1, F_2 and F_3, the TED in the first (second) vibration mode of the SiC resonator is lower by ~3.2% (~6.9%). This is important if the resonator is used for detecting deposition on it of tiny either dust particles or biological agents.

For $\lambda = 5$ and 10 and the beam vibrating in the first mode, we have exhibited in Fig. 2 the dependence of Q^{-1} upon beam's thickness h. The computed values of Q^{-1} for the three shear deformation functions are nearly the same, however, their peak values noticeably differ from that for the EBBT. Defining the relative error as, $r = (Q_E^{-1} - Q_L^{-1})/Q_E^{-1}$, where subscripts E and L, respectively, denote the E–B ($F = 0$) and the Levinson ($F = F_2$) beam theories, the maximum value $r_{\max}$ of r equals 2.3% and 8.2%, respectively, for $\lambda = 10$ and $\lambda = 5$ for the SiC beam, and 2.6% and 9.0% for the Ni beam. In each case, they occur for different values of the beam thickness.

In Fig. 3 we have depicted for $\lambda = 5$ and the first three vibration modes the Q^{-1} versus $\log_{10}(\omega_{E0})$ for the two beams where ω_{E0} is the isothermal natural frequency computed using the EBBT. It is found that for the 1st, 2nd and the 3rd modes $r_{\max}$ equals, respectively, 2.3%, 8.1%, and 15.8% for the Si beam and 2.6%, 9.0% and 17.3% for the Ni beam. Thus, effects of shear deformation on the TED are more in higher modes of vibration.

Recalling that thermal coupling in the heat equation is proportional to the initial temperature T_0, we have displayed in Fig. 4 for three values of T_0 the dependence of Q^{-1} upon the SiC beam thickness for aspect ratio $\lambda = 10$ and 5. As expected for a fixed thickness of the beam Q^{-1} increases monotonically with an increase in T_0. We could not analytically solve the problem and derive closed-form expressions for the quality factor when material properties depend upon the temperature. Our values of Q^{-1} at the three temperatures, 150, 200 and 300 K should be illustrative of qualitative trends rather than as exact values.

We have delineated in Fig. 5 the effect of the energy dissipation upon the frequency shift, $(\mathrm{Re}(\Omega) - \Omega_0)/\Omega_0$, and the attenuation,

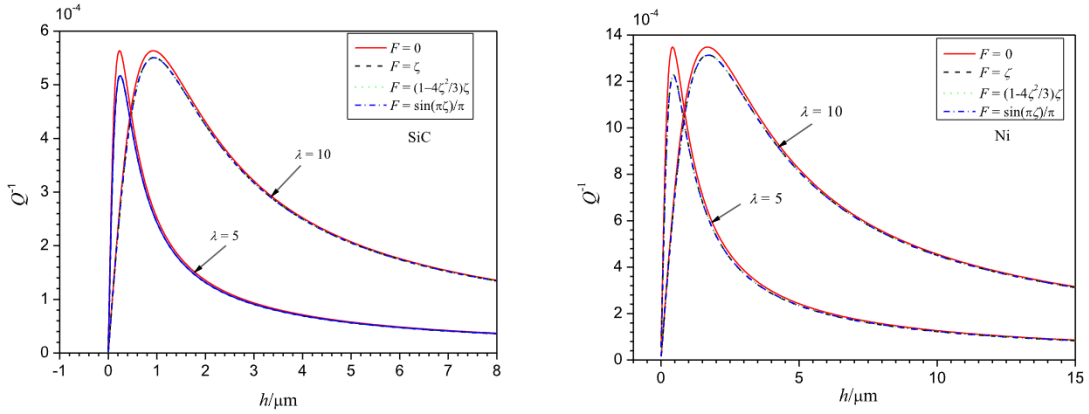

Fig. 2. For $\lambda = 5, 10$ and beams vibrating in the 1st mode the dependence of Q^{-1} upon the beam thickness for three shear deformation functions (1st mode); (left) SiC beam, and (right) Ni beam.

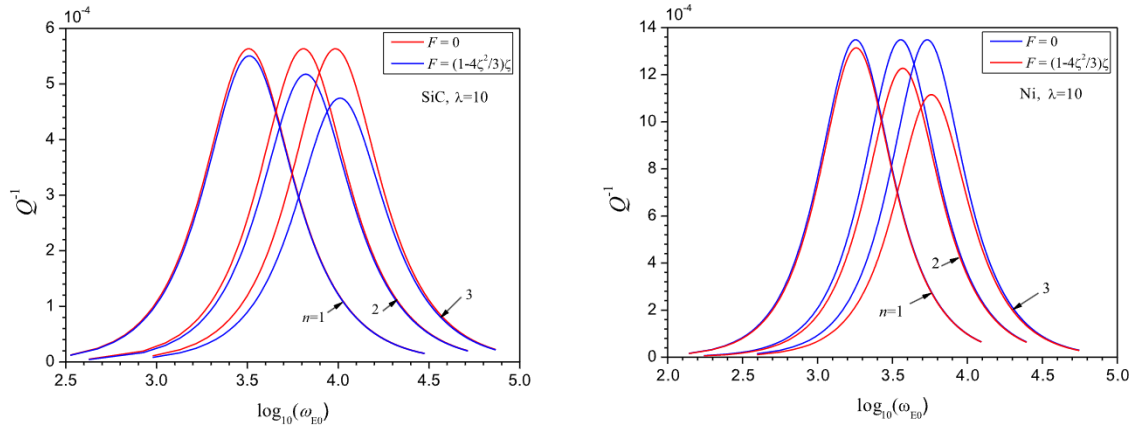

Fig. 3. For the first three vibration modes and $\lambda = 10$, the dependence of Q^{-1} upon $\log_{10}(\omega_0)$ for the two beams using the EBBT and the Levinson beam theory; (left) SiC beam, and (right) Ni beam.

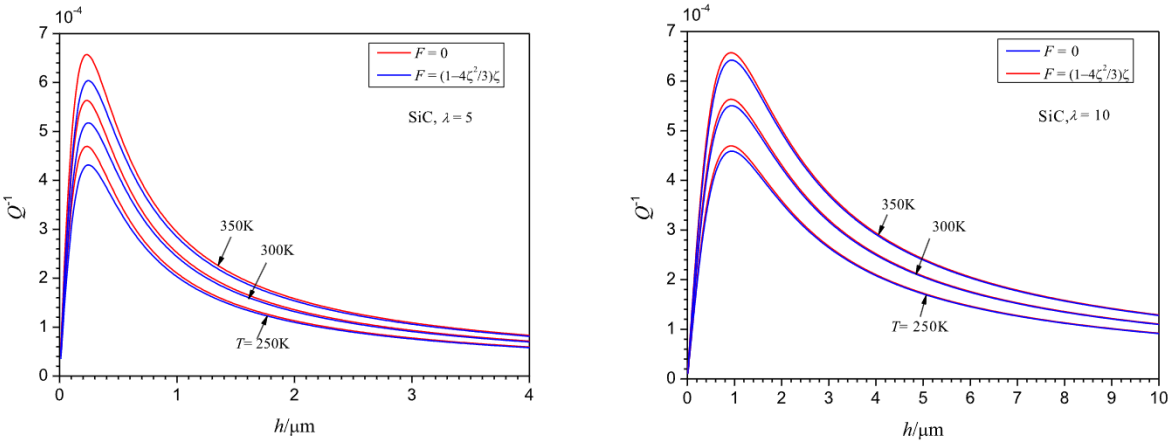

Fig. 4. For the SiC beam vibrating in the 1st mode at $T_0 = 250$ K, 300 K and 350 K and using the E–B and the Levinson beam theories the dependence of Q^{-1} upon the beam thickness; (left) $\lambda = 5$, and (right) $\lambda = 10$.

$\mathrm{Im}(\Omega)/\Omega_0$, for SiC beams of different thicknesses having $\lambda = 10$ and 7. It is evident that the consideration of the shear deformation shifts the frequency more than it affects the attenuation.

Finally, Fig. 6 shows through-the-thickness variation of the temperature rise, defined by $\tau_i(\zeta) = \mathrm{Re}[H_i(\zeta)]/\alpha$ for the SiC and the Ni beams with $\lambda = 10$ and 5 predicted by different beam theories. It can be seen that the temperature rise predicted by the shear deformation theories are less than that by the EBBT. Moreover, comparing results for the two values of λ, the difference is higher for the beam with $\lambda = 5$. However, the differences between the temperature rise estimated by the three shear deformation functions are negligible. Furthermore, the temperature distribution in an isotropic and homogeneous resonator is antisymmetric about its geometric mid-surface similar to the distribution of the normal stress. Recall that the TED is proportional to the dilatation that has opposite sign at points above and below the mid-surface.

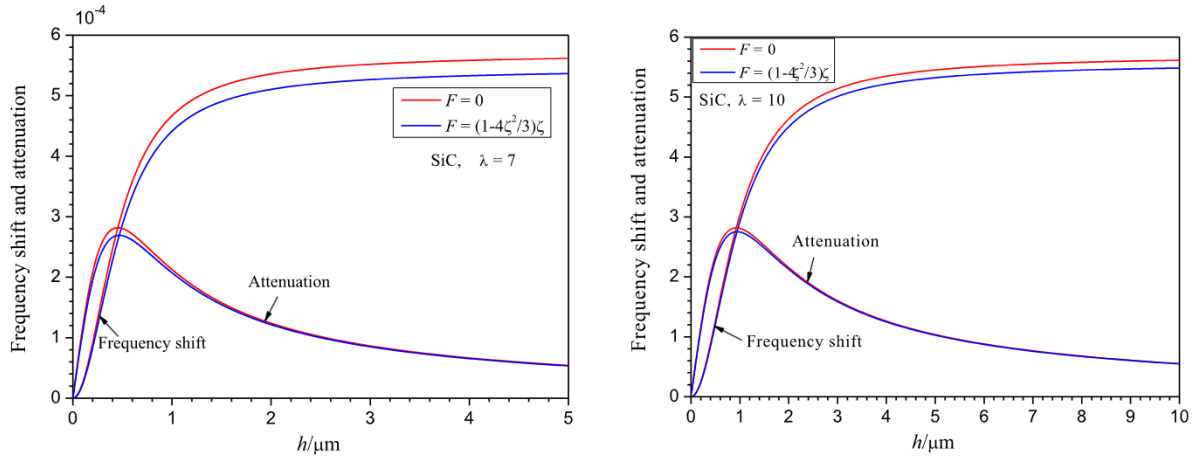

Fig. 5. Frequency shift and attenuation versus the thickness of the SiC beam vibrating in the 1st mode using the E–B and the Levinson beam theories; (left) $\lambda = 7$, and (right) $\lambda = 10$.

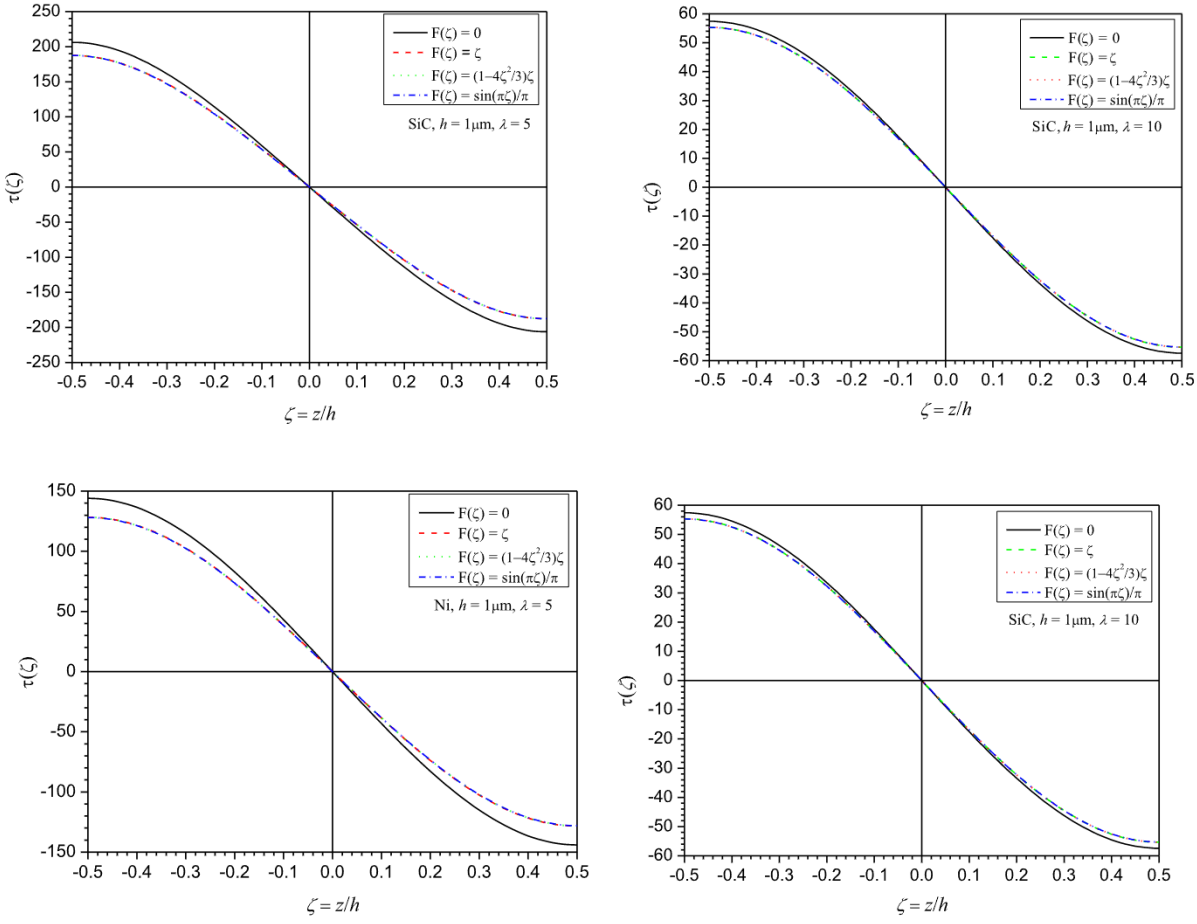

Fig. 6. Through-the-thickness variation of the dimensionless temperature $\tau(\zeta)$ change for 1 μm thick (top) SiC and (bottom) Ni beams vibrating in the 1st mode.

8. Conclusions

We have analytically quantified the thermo-elastic damping (TED) in high frequency vibrations of a simply-supported beam of rectangular cross-section using three through-the-thickness distributions of the shear stress, namely, linear, cubic polynomial and sinusoidal functions of the thickness coordinate. Assuming that the heat conduction is dominant in the thickness direction, we have also derived through-the-thickness variation of the temperature in the beam. An important result is the closed-form expressions for the first three complex frequencies of the beam resonators, and the inverse quality factors for them. The quality factor measures the percentage shift in the frequency caused

by the thermo-elastic damping (TED). For three through-the-thickness variations of the shear stress, numerical results for different values of the aspect ratio (length/thickness), initial temperature, and beam thickness having the same aspect ratio are presented. These lead us to the following conclusions.

(a) Eqs. (40) and (41) express the frequency of a shear deformable beam in terms of that of a Euler–Bernoulli beam and provide better estimates of the TED than that given by the EBBT.
(b) The effect of the shear deformation on the TED becomes significant with a decrease in beam's aspect ratio, and for a given aspect ratio is nearly the same for the three through-the-thickness shear deformations considered.
(c) Like the axial stress and the axial strain, the through-the-thickness temperature distribution is asymmetric about the beam's mid-surface.

The work can be extended to beams with other boundary conditions, and considering other heat conduction and non-local theories.

CRediT authorship contribution statement

Shi-Rong Li: Conceptualization. **Feng Zhang:** Formal analysis. **R.C. Batra:** Writing – review & editing.

Declaration of competing interest

The authors declare that they have no known competing financial interests or personal relationships that could have appeared to influence the work reported in this paper.

Data availability

No data was used for the research described in the article.

Acknowledgment

The first author gratefully acknowledges the financial support from the National Natural Science Foundation of China grant number 11672260.

Data deposition

All relevant data used in the article is included in the manuscript.

References

[1] W. Nowacki, Thermoelasticity, second ed., PWN-Polish Scientific Publishers, Warszawa, 1986, pp. 1–50, revised and enlarged.
[2] C. Zener, Internal friction in solids. I. Theory of internal fraction in reeds, Phys. Rev. 52 (1937) 230–235.
[3] C. Zener, Internal friction in solids. II. General theory of thermoelastic internal friction, Phys. Rev. 53 (1938) 90–99.
[4] J.E. Bishop, V.K. Kinra, Thermoelastic damping of a laminated beam in flexure and extension, J. Reinf. Plast. Compos. 12 (1993) 210–217.
[5] J.E. Bishop, V.K. Kinra, Equivalence of the mechanical and entropic description of elasto-thermodynamics in composite materials, Mech. Compos. Mater. Struct. 3 (1996) 83–95.
[6] S. Prabhakar, S. Vengallatore, Theory of thermo-elastic damping in micromechanical resonators with two-dimensional heat conduction, J. Micromech. Syst. 17 (2008) 494–502.
[7] W.L. Zuo, P. Li, J.K. Du, Z.T.H. Tse, Thermoelastic damping in anisotropic piezoelectric microbeam resonators, Int. J. Heat Mass Transfer 199 (2022) 123493.
[8] S. Vengallatore, Analysis of thermoelastic damping in laminated composite micromechanical beam resonators, J. Micromech. Microeng. 15 (2005) 2398–2404.
[9] S. Prabhakar, S. Vengallatore, Thermoelastic damping in bilayered micromechanical beam resonators, J. Micromech. Microeng. 17 (2007) 532–538.
[10] W.L. Zuo, P. Li, Y.M. Fang, J.R. Zhang, Thermoelastic damping in asymmetric three-layered microbeam resonators, J. Appl. Mech. 83 (2016) 061002-1.
[11] L.F. Yang, P. Li, Y.M. Fang, H.Y. Zhou, Thermoelastic damping in bilayer microbeam resonators with two-dimensional heat conduction, Int. J. Mech. Sci. 167 (2020) 105245.
[12] L.F. Yang, P. Li, Y.M. Fang, X. Ce, Thermoelastic damping in partially covered bilayer microbeam resonators with two-dimensional heat conduction, J. Sound Vib. 394 (2021) 115863.
[13] H. Zhou, P. Li, Thermoelastic damping in micro- and nano-beam resonators with non-Fourier heat conduction, IEEE Sens. J. 17 (2017) 6966–6977.
[14] H. Kumar, S. Mukhopadhyay, Thermoelastic damping in micro and nano-mechanical resonators utilizing entropy generation approach and heat conduction model with single delay term, Int. J. Mech. Sci. 165 (2020) 105211.
[15] S.H. Shi, F. Jin, T.H. He, F.T. Shi, Thermoelastic damping analysis model of transversely isotropic micro/nano-resonators based on dual-phase-lag heat conduction model and surface effect, Compos. Struct. 292 (2022) 115664.
[16] D.V. Parayil, S.S. Kulkarni, N. Pawaskar, Analytical and numerical solutions for thick beams with thermoelastic damping, Int. J. Mech. Sci. 94–95 (2015) 10–19.
[17] D.V. Parayil, S.S. Kulkarni, D.N. Pawaskar, A generalized model for thermoelastic damping in beams with mid-plane stretching nonlinearity, Int. J. Mech. Sci. 135 (2018) 582–595.
[18] R. Lifshitz, M.L. Roukes, Thermo-elastic damping in micro- and nano-mechanical system, Phys. Rev. B 61 (2000) 5600–5609.
[19] G. Rezazadeh, A.S. Vahdat, S. Tayefeh-Rezaei, C. Cetinkaya, Thermo-elastic damping in a micro-beam resonator using modified couple stress theory, Acta Mech. 223 (2012) 1137–1152.
[20] R. Resmi, S.V. Babu, M.R. Baiju, Material-dependent thermoelastic damping limited quality factor and critical length analysis with size effects of micro/nanobeams, J. Mech. Sci. Technol. 36 (2022) 3017–3018.
[21] A. Khanchehgardan, G. Rezazadeh, R. Shabani, Effect of mass diffusion on the damping ratio in a functionally graded micro-beam, Compos. Struct. 106 (2013) 15–29.
[22] S. Azizi, M.R. Ghazavi, G. Rezazadeh, S.E. Khadem, Thermo-elastic damping in a functionally graded piezoelectric micro-resonator, Int. J. Mech. Mater. Des. 11 (2015) 357–369.
[23] Z.Y. Zhong, J.P. Zhou, H.L. Zhang, Thermoelastic damping in functionally graded microbeam resonators, IEEE Sens. J. 17 (2017) 3381–3390.
[24] S.R. Li, X. Xu, S. Chen, Analysis of thermoelastic damping of functionally graded material beam resonators, Compos. Struct. 182 (2017) 728–736.
[25] Z.C. Zhang, S.R. Li, Thermoelastic damping of functionally graded material microbeam resonators based on the modified couple stress theory, Acta Mech. Solida Sin. 33 (2020) 496–507.
[26] Y.B. Yi, M.A. Martin, Eigenvalue solution of thermoelastic damping in beam resonators using finite element analysis, J. Vib. Acoust. 129 (2007) 478–482.
[27] C. Mendez, S. Paquay, I. Klapka, J.P. Raskin, Effects of geometrical nonlinearity on MEMS thermoelastic damping, Nonlinear Anal. Real World Appl. 10 (2009) 1579–1588.
[28] X. Guo, Y.B. Yi, S. Pourkamali, A finite element analysis of thermoelastic damping in vented MEMS beam resonators, Int. J. Mech. Sci. 74 (2013) 73–82.
[29] Guo. X, YB. Yi, Suppression of thermoelastic damping in MEMS beam resonators by piezoresistivity, J. Sound Vib. 333 (2014) 1079–1095.
[30] R.J. Cheng, P.C. Song, J.X. Chen, Q.X. Huang, L.S. Zhang, Thermoelastic damping suppression method of micro-beam resonators with basically constant resonant frequency, J. Therm. Stress. 45 (2022) 960–973.
[31] A. Kar, M. Kanoria, Generalized thermoelastic functionally graded orthotropic hollow sphere under thermal shock with three-phase-lag effect, Eur. J. Mech. A Solids 28 (2009) 757–767.
[32] F.L. Guo, Thermoelastic dissipation of microbeam resonators in the framework of generalized thermos-elasticity theory, J. Therm. Stress. 36 (2013) 1156–1168.
[33] F.L. Guo, W.J. Jiao, G.Q. Wang, Z.Q. Chen, Distinctive features of thermoelastic dissipation in microbeam resonators at nanoscale, J. Therm. Stress. 39 (2016) 360–369.
[34] I.A. Abbas, A two temperature model for evaluation of thermoelastic damping in the vibration of a nanoscale resonators, Mech. Time Dependent Mater. 20 (2016) 511–522.
[35] H.M. Youssef, A.A. El-Bary, The reference temperature dependence of Young's modulus of two-temperature thermoelastic damping of gold nano-beam, Mech. Time-Depend Mater. 22 (2018) 435–445.
[36] S.A. Vahdat, G. Rezazadeh, G. Ahmadi, Thermoelastic damping in a micro-beam resonator tunable with piezoelectric layers, Acta Mech. Solida Sin. 25 (2012) 73–81.
[37] M. Bostani, A.K. Mohammadi, Thermoelastic damping in microbeam resonators based on modified strain gradient elasticity and generalized thermoelasticity theories, Acta Mech. 229 (2018) 173–192.
[38] H. Kumar, S. Mukhopadhyay, Analysis of the quality factor of micro-beam resonators based on heat conduction with single delay term, J. Therm. Stress. 42 (2019) 929–942.
[39] R. Kumar, R. Kumar, Effects of phase-lags on thermoelastic damping in micromechanical resonators, J. Therm. Stress. 41 (2018) 1115–1124.
[40] R. Kumar, R. Kumar, A study of thermoelastic damping in micromechanical resonators under unified generalized thermoelasticity formulation, Noise Vib. Worldwide 50 (2019) 169–175.

[41] R. Kumar, R. Kumar, Significance of memory-dependent derivative approach for the analysis of thermoelastic damping in micromechanical resonators, Mech. Time-Dependent Mater. 26 (2022) 101–118.
[42] V. Borjalilou, M. Asghari, E. Bghari, V. Borjalilou, M. Asghari, E. Taati, Small-scale thermoelastic damping in micro-beams utilizing the modified couple stress theory and the dual-phase-lag heat conduction model, J. Therm. Stress. 42 (2019) 801–814.
[43] V. Borjalilou, M. Asghari, Size-dependent analysis of thermoelastic damping in electrically actuated microbeams, Mech. Adv. Mater. Struct. 28 (2021) 952–962.
[44] S. Guha, A.K. Singh, Frequency shifts and thermoelastic damping in different types of nano-/micro-scale beams with sandiness and voids under three thermoelasticity theories, J. Sound Vib. 510 (2021) 116301.
[45] I. Kaur, P. Lata, K. Singh, Study of frequency shift and thermoelastic damping in transversely isotropic nano-beam with GN III theory and two temperatures, Arch. Appl. Mech. 91 (2021) 1697–1711.
[46] H. Kumar, S. Mukhopadhyay, Size-dependent thermoelastic damping analysis in nanobeam resonators based on Eringen's nonlocal elasticity and modified couple stress theories, J. Vib. Control 29 (7–8) (2023) 1510–1523.
[47] V. Borjalilou, M. Asghari, E. Taati, Thermoelastic damping in nonlocal nanobeams considering dual-phase-lagging effect, J. Vib. Control 26 (2020) 1042–1053.
[48] I. Kaur, P. Lata, K. Singh, Thermoelastic damping in generalized simply supported piezo-thermo-elastic nanobeam, Struct. Eng. Mech. 81 (2022) 29–37.
[49] B.D. Gu, S.H. Shi, Y.B. Ma, T.H. He, Thermoelastic damping analysis in nanobeam resonators considering thermal relaxation and surface effect based on the nonlocal strain gradient theory, J. Therm. Stress. 45 (2022) 974–992.
[50] G. Rezazadeh, M. Seikhlou, Analysis of bias DC voltage effects on thermoelastic damping ratio in short nano-beam resonators based on nonlocal elasticity theory and dual-phase-lagging heat conduction, Mechanica 50 (2015) 2963–2976.
[51] A.A. Emami, A. Alibeigloo, Exact solution for thermal damping of functionally graded Timoshenko microbeams, J. Therm. Stress. 39 (2016) 231–243.
[52] K. Tunvir, C. Ru, A. Mioduchowski, Effects of cross-sectional shape on thermoelastic dissipation of micro/nano elastic beams, Int. J. Mech. Sci. 62 (2012) 77–88.
[53] J.S. Yang, R.C. Batra, Free vibrations of a linear thermo-piezoelectric body, J. Therm. Stress. 18 (1995) 247–262.
[54] A.C. Eringen, On differential equations of nonlocal elasticity and solutions of screw dislocation and surface waves, J. Appl. Phys. 54 (1983) 4703–4710.
[55] R.C. Batra, On heat conduction and wave propagation in non-simple rigid solids, Lett. Appl. Eng. Sci. 3 (1975) 97–107.
[56] C. Cattaneo, A form of heat equation which eliminates the paradox of instantaneous propagation, CR Acad. Sci. 247 (1958) 431–433.
[57] M. Chester, Second sound in solids, Phys. Rev. 131 (1963) 2103–2105.
[58] X. Wang, S.R. Li, Free vibration analysis of functionally graded material beams based on Levinson beam theory, Appl. Math. Mech. (English Ed.) 37 (2016) 861–878.
[59] A.S. Sayyad, Y.M. Ghugal, Modeling and analysis of functionally graded sandwich beams: A review, Mech. Adv. Mater. Struct. 26 (2019) 1776–1795.
[60] Y.M. Xia, S.R. Li, Z.Q. Wan, Bending solutions of FGM Reddy-Bickford beams in terms of those of the homogenous Euler–Bernoulli beams, Acta Mech. Solida Sin. 32 (2019) 393–420.
[61] A. Pydah, R.C. Batra, Shear deformation theory using logarithmic function for thick circular beams and analytical solution for bi-directional functionally graded circular beams, Compos. Struct. 172 (2017) 45–60.
[62] L.F. Qian, R.C. Batra, L.M. Chen, Elastostatic deformations of a thick plate by using a higher-order shear and normal deformable plate theory and two meshless local Petrov–Galerkin (MLPG) methods, Comput. Model. Eng'g Sci. 4 (2003) 161–176.
[63] R.C. Batra, S. Vidoli, Higher order piezoelectric plate theory derived from a three-dimensional variational principle, AIAA J. 40 (2002) (2002) 91–104.
[64] E. Carrera, V.V. Zozulya, Carrera unified formulation (CUF) for the micropolar plates and shells, I. Higher order theory, Mech. Adv. Mater. Struct. 29 (2022) http://dx.doi.org/10.1080/15376494.2020.1793241.
[65] A. Entezari, M. Filippi, E. Carrera, Unified finite element approach for generalized coupled thermoelastic analysis of 3D beam-type structures, part 1: Equations and formulation, J. Therm. Stress. 40 (2017) 1386–1401.
[66] R.C. Batra, S. Vidoli, F. Vestroni, Plane waves and modal analysis in higher-order shear and normal deformable plate theories, J. Sound Vib. 257 (2002) (2002) 63–88.
[67] R.D. Mindlin, An Introduction to the Mathematical Theory of Vibrations of Elastic Plates (Ed. Jiashi Yang), World Scientific, Publishing Co. NJ, 2006.
[68] L.F. Qian, R.C. Batra, Transient thermoelastic deformations of a thick functionally graded plate, J. Therm. Stress. 27 (2004) 705–740.
[69] M. Ayada, N. Karathanasopoulos, J.F. Ganghoffer, H. Lakiss, Higher-gradient and micro-inertia contributions on the mechanical response of composite beam structures, Internat. J. Engrg. Sci. 154 (2020) 103318.